Sub-Array-Based Millimeter Wave Massive MIMO Channel Estimation

Xuan Zhu[ID], Yang Liu[ID], and Cheng-Xiang Wang[ID]

Abstract—Combination of millimeter wave (mmWave) and massive multiple input multiple output (MIMO) forms a promising technology for future sixth generation networks. As the number of antennas increases, propagation channel starts yielding spherical wavefronts, for which the traditional channel estimation algorithms are no longer applicable. To overcome this technical gap, a novel MIMO channel estimation scheme based on the assumption of spherical wavefront is proposed in this letter. The large antenna array is first divided into several sub-arrays, and then the channel estimation is performed for each sub-array based on the orthogonal matching pursuit algorithm. In addition, the joint estimation of angle of arrivals and departures (AoAs and AoDs) of each uniform planar sub-array is transformed into separate estimation by dimensionality reduction. Next, an iterative estimation is performed using Taylor expansion to continuously approximate the real grid points to recover the AoAs/AoDs. Lastly, the superiority of the proposed algorithm is verified by numerical simulations, where the proposed algorithm exhibits the best NMSE performance, compared with the existing MIMO channel estimation methods.

Index Terms—Massive MIMO, channel estimation, sub-array, spherical wave, off-grid error.

I. INTRODUCTION

MASSIVE multiple input multiple output (MIMO) technologies are being effectively exploited in the fifth generation (5G) and the sixth generation (6G) wireless communication systems [1], [2]. Meanwhile, millimeter-wave (mmWave) communication has been proposed for 5G and 6G cellular networks to enhance the spectrum efficiency [3], [4]. Accordingly, a combination of mmWave communication and massive MIMO technologies has promised to provide higher data rate, throughput, and capacity in the future communication systems [5], [6]. To achieve the desired performance, accurate acquisition of channel state information (CSI) is crucial for the mmWave and massive MIMO systems [7].

Study on the channel estimation algorithms can be traced back to [8], where a Gaussian channel was estimated by the likelihood function method. Over the past decades, various research groups have intensively studied the estimation algorithms for massive MIMO channel. Generally, these reported algorithms could be divided into two categories. Among them, the first type relies on the plane wave model (PWM). In [9], algorithm based on the alternating direction method of multipliers (ADMM) for the mmWave channel was proposed by taking advantage of the channel sparsity and low rank. In [10], orthogonal matching pursuit (OMP) algorithm was proposed to estimate the mmWave channel. Progressively, in [11], a two-dimensional unitary ESPRIT-based algorithm was proposed to estimate the MIMO channel at mmWave bands. In [12], a two-stage grid estimation method was proposed, where the first stage was to obtain a general grid. Next, the second stage performed a detailed division of the grid, to obtain the specific CSI. In [13], algorithm based on analog beamforming was proposed, which can significantly improve the gain and reduce the overhead.

To reduce the complexity, the antenna array can be divided into several sub-arrays, and each sub-array can be estimated independently. Reference [14] estimated angles of arrival/departure (AoAs/AoDs) based on the gradient descent method. However, these results included the off-grid errors. Correspondingly, [15] proposed a solution for the off-grid errors by converting the joint estimation of AoAs/AoDs into a separate estimate. Reference [16] considered both azimuth and elevation angles. Moreover, for a large number of antennas, the spatial non-stationarity (SNS) caused by the cluster appearance and disappearance along the array was addressed in [17]. Notably, such SNS of the massive MIMO channel was not considered in the traditional algorithms. Then, [18] proposed a block matching pursuit algorithm to estimate those channels. In [19], an end-to-end (E2E) joint training method based on deep learning (DL) is proposed. However, the above-mentioned algorithms did not fully support the spherical wave model (SWM).

Later on, the second type of MIMO channel estimation algorithms were put forward, which relied on the assumption of SWM based propagation. When the distance between the receiver and transmitter ends is less than the Rayleigh distance, propagation channel possesses the property of spherical wavefront. Reference [20] proposed a channel estimation algorithm based on intermediate parabolic wavefront. Reference [21] proposed an algorithm to estimate the near-field components
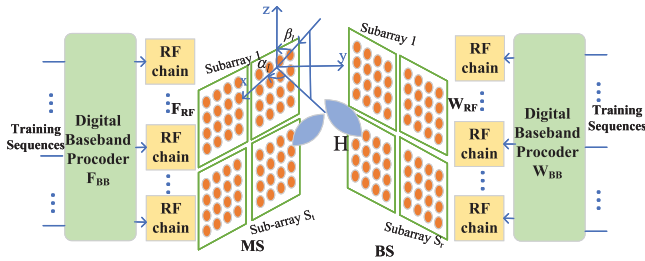
Fig. 1. Structure diagram of hybrid precoding massive MIMO multi-antenna system, the azimuth angle α_l and elevation angle β_l.

based on simultaneously OMP algorithm in the polar domain. However, only near-field channels can be estimated and far-field channels were ignored. Furthermore, [22] proposed a hybrid-field algorithm to estimate both the far-field and near-field components. Reference [23] proposed a spherical wave channel estimation scheme using deep convolutional neural network in terahertz scenario. Reference [24] proposed a hybrid channel estimation scheme by dividing a large array into several small sub-arrays. But the above methods did not consider the off-grid error, which may lead to the significant error of the estimated channel.

To the best of our knowledge, an algorithm for the spherical channel with small off-grid errors is still missing. To fill this gap, a scheme to solve the off-grid error problem of estimating the massive MIMO channel with the spherical wavefront is proposed in this letter. The main contributions of this letter include the estimation of channel parameters between each sub-array separately using a parallel approach. Additionally, the joint estimation of AoAs and AoDs is transformed into separate estimation to achieve dimensionality reduction. In addition, Taylor expansion formula is used to reduce the off-grid error, so that the estimated angle is close to the real angle.

The rest of this letter is organized as follows. The system and channel model are illustrated in Section II. In Section III, we propose a novel channel estimation scheme based on the SWM. Section IV evaluates the performance of the proposed algorithm by Monte Carlo simulations. Finally, Section V summarizes this letter.

II. HYBRID MIMO SYSTEM AND CHANNEL MODEL

Fig. 1 presents a massive MIMO communication scenario with N_t (N_r) antennas at the transmitter (receiver). Uniform planar array (UPA) is employed at both transmitted and received ends. This letter mainly focus on the uplink, the received signal can be expressed as [11]:

$$\mathbf{Y} = \mathbf{W}^{\mathrm{H}}(\mathbf{H}\mathbf{F}\mathbf{X} + \mathbf{N}) \tag{1}$$

where $\mathbf{W} = \mathbf{W}_{\mathrm{RF}}\mathbf{W}_{\mathrm{BB}} \in \mathbb{C}^{N_r \times N_x}$ is the hybrid combiner, $\mathbf{F} = \mathbf{F}_{\mathrm{RF}}\mathbf{F}_{\mathrm{BB}} \in \mathbb{C}^{N_t \times N_x}$ is the hybrid precoder. $\mathbf{H} \in \mathbb{C}^{N_r \times N_t}$ is the channel matrix, $\mathbf{X} \in \mathbb{C}^{N_x \times N_x}$ is the matrix of transmitted pilot signals. Meanwhile, $\mathbf{N} \in \mathbb{C}^{N_r \times N_x}$ is the additive zero mean Gaussian noise with variance σ_n^2.

Our proposed algorithm is based on the non-line-of-sight (NLOS) propagation [25]. In the spherical wave model, each

element of the channel matrix represents the channel impulse response between the ith received antenna and the kth transmitted antenna, expressed as [23]:

$$(\mathbf{H})_{ik} = \sum_{l=1}^{L} \left| \mu_l^{ik} \right| e^{-j 2\pi d_l^{ik}/\lambda} \tag{2}$$

where $l = 1, 2, \ldots L$ indicates the propagation path between the transmitted and received antenna pairs. μ_l^{ik}, d_l^{ik} denotes the complex channel gain and the communication distance of the lth path between the ith received antenna and the kth transmitted antenna, respectively.

III. CHANNEL ESTIMATION

In this section, based on the OMP, a hybrid pre-coded channel estimation scheme for the massive MIMO channel at mmWave bands is proposed. First, the large arrays of transmitter and receiver ends are divided into several sub-arrays. A sparse signal reconstruction scheme is then used to initial the sparse support set of each sub-array. Next, Taylor expansion is used to iteratively find the grid points closest to AoAs and AoDs of each sub-array. Later, the least square method is used to estimate the path gain. Finally, according to the obtained AOAs, AoDs and path gain of each sub-array, the channel matrix of the large array is reconstructed.

A. Partitioning the Sub-Array

In this letter, the spherical wavefront property of massive MIMO channel is considered, we divide the large-scale arrays at the transmitter and receiver into S_t and S_r subarrays, respectively. Each sub-array at the z end has $N_{S_z} = N_z/S_z$ antennas ($z = t, r$). Thus, the propagation channel between the small subarrays of the transmitted and received ends may be assumed to possess the plane wavefront. The channel matrix between the pth ($p = 1, 2, \ldots S_r$) received sub-array and the qth ($q = 1, 2, \ldots S_t$) transmitted sub-array at mmWave band can be written as [15]:

$$\begin{aligned}
\mathbf{H}_{sub}^{pq} &= \mathbf{A}_r^p \operatorname{diag}(\boldsymbol{\mu}^{pq}) \mathbf{A}_t^{qH} \\
&= \sqrt{\frac{N_{S_t} \times N_{S_r}}{L}} \sum_{l=1}^{L} \mu_l^{pq} \mathbf{a}_{rl}^p(\alpha_{rl}^p, \beta_{rl}^p) \mathbf{a}_{tl}^q(\alpha_{tl}^q, \beta_{tl}^q)^H
\end{aligned} \tag{3}$$

where $\operatorname{diag}(\cdot)$ represents diagonal operation and $\boldsymbol{\mu}^{pq} = (\mu_1^{pq}, \ldots, \mu_L^{pq})$. μ_l^{pq} is the gain of lth path between the pth received sub-array and the qth transmitted sub-array, $\mathbf{A}_r^p = [\mathbf{a}_{r1}^p(\alpha_{r1}^p, \beta_{r1}^p), \ldots, \mathbf{a}_{rL}^p(\alpha_{rL}^p, \beta_{rL}^p)] \in \mathbb{C}^{N_{S_r} \times L}$ represents the received array response matrix. $\mathbf{A}_t^q = [\mathbf{a}_{t1}^q(\alpha_{tq}^1, \beta_{tq}^1), \ldots, \mathbf{a}_{tL}^q(\alpha_{tL}^q, \beta_{tL}^q)] \in \mathbb{C}^{N_{S_t} \times L}$ stands for the transmitted array response matrix. For the pth received sub-array, $\alpha_{rl}^p, \beta_{rl}^p$ denote the azimuth and elevation AoAs of the lth path, respectively. Similarly, $\alpha_{tl}^q, \beta_{tl}^q$ represent the azimuth and elevation AoDs of the lth path of the qth transmitted sub-array. $\mathbf{a}_{rl}^p(\alpha_{rl}^p, \beta_{rl}^p)$ denotes the response vector of the pth received sub-array, which can be expressed as:

$$\mathbf{a}_{rl}^p(\alpha_{rl}^p, \beta_{rl}^p) = \left[1, \ldots, e^{j 2\pi \Delta d (N_{r1}-1) \sin \alpha_{rl}^p \sin \beta_{rl}^p / \lambda} \right]^T$$

$$\otimes \left[1, \ldots, e^{j2\pi\Delta d(N_{r2}-1)\cos\beta_{rl}^p/\lambda} \right]^T \quad (4)$$

where $\otimes$ denotes the Kronecker product, Δd represents the spacing between antennas, N_{r1} and N_{r2} represent the number of antennas of the pth sub-array in the horizontal and vertical, respectively. Similarly, the response vector of the qth transmitted sub-array $\mathbf{a}_{tl}^q$ can be obtained.

The full MIMO spherical wave channel matrix can be obtained by combining model (2) and model (3) (the bottom of the page).

B. Optimizing and Reconstructing the Received Signal

The transmitted signal $\mathbf{X}$ is assumed to be a unitary matrix($\mathbf{XX}^H = \mathbf{I}_{N_x}$). Eq. (1) is multiplied by $\mathbf{X^T}$ on both sides, the equivalent received signal can be expressed:

$$\hat{\mathbf{Y}}_{pq} = \hat{\mathbf{A}}_r^p \, \mathrm{diag}(\boldsymbol{\mu}^{pq})\hat{\mathbf{A}}_t^q + \hat{\mathbf{N}} \quad (6)$$

where $\hat{\mathbf{A}}_r^p = \mathbf{W}^H\mathbf{A}_r^p$, $\hat{\mathbf{A}}_t^q = \mathbf{A}_t^{qH}\mathbf{F}$ are the equivalent channel response matrices, and $\hat{\mathbf{N}} = \mathbf{W}^H\mathbf{N}\mathbf{X}^H$ is the noise matrix. By vectorizing both sides of Eq. (6), we get

$$\hat{\mathbf{y}}^{pq} = \mathrm{vec}\left(\hat{\mathbf{Y}}^{pq}\right) = \hat{\mathbf{A}}^{pq}\mathbf{u}^{pq} + \hat{\mathbf{n}} \quad (7)$$

where $\hat{\mathbf{A}}^{pq} = \hat{\mathbf{A}}_r^p \odot \hat{\mathbf{A}}_t^{q*}$, $\mathbf{u}^{pq} = \mathrm{vec}(\mathrm{diag}(\boldsymbol{\mu}^{pq}))$, $\hat{\mathbf{n}} = \mathrm{vec}(\hat{\mathbf{N}})$.

The optimal model of the signal can be established:

$$\min\|\mathbf{u}^{pq}\|_0, s.t. \left\|\hat{\mathbf{y}}^{pq} - \hat{\mathbf{A}}^{pq}\mathbf{u}^{pq}\right\|_F^2 \leq \varepsilon \quad (8)$$

where ε is the error tolerance parameter.

To reduce the computational complexity, a parallel scheme is used to reconstruct Eq. (7)

$$\hat{\mathbf{y}}^{pq} = \begin{bmatrix} \hat{\mathbf{A}}_r^p \, \mathrm{diag}\left(\mathbf{A}_t^{q*}\right)_1 \\ \cdots \\ \hat{\mathbf{A}}_r^p \, \mathrm{diag}\left(\mathbf{A}_t^{q*}\right)_{N_x/S_t} \end{bmatrix} \mathbf{u}^{pq} + \hat{\mathbf{n}} \quad (9)$$

where $\mathrm{diag}(\cdot)_i$ diagonalizes the ith row of matrix $(\cdot)$.

According to Eq. (9), the AoA-dependent signal model between the pth received sub-array and the qth transmitted sub-array can be obtained.

$$\mathbf{X}_r^{pq} = \hat{\mathbf{A}}_r^p \begin{bmatrix} \mathrm{diag}\left(\mathbf{A}_t^{q*}\right)_1 \mathbf{u}_{pq} \\ \cdots \\ \mathrm{diag}\left(\mathbf{A}_t^{q*}\right)_{N_x/S_t} \mathbf{u}_{pq} \end{bmatrix}^T + \hat{\mathbf{N}}_r \quad (10)$$

where $\hat{\mathbf{N}}_r$ is the noise term. Similarly, the AoD-dependent signal model between the pth received sub-array and the qth transmitted sub-array $\mathbf{X}_t^{pq}$ can be obtained. Thus the AoAs and the AoDs can be separated.

C. Reducing the Off-Grid Errors and Recovering the Channel Matrix

We perform the singular value decomposition (SVD) on the AoD-dependent signal model $\mathbf{X}_t^{pq} = \mathbf{U}_{pq}\Sigma_{pq}\mathbf{V}_{pq}^H$ to distinguish the signal from the noise. To extract the information of AoDs, we select the first L columns of $\mathbf{V}_{pq}$ defined as $\mathbf{V}_{pq}^L$. Thus the signal subspace can be expressed as $\mathbf{X}_{sv}^{pq} = \mathbf{X}_t^{pq}\mathbf{V}_{pq}^L$, and then calculate its orthogonal projection matrix $\mathbf{E}_t^{pq} = \mathbf{I} - \mathbf{X}_t^{pq}(\mathbf{X}_t^{pq^H}\mathbf{X}_t^{pq})^{-1}\mathbf{X}_t^{pq^H}$.

Due to non-continuity and non-convexit, Eq. (8) is relatively difficult to solve. Therefore, we perform $l1$-norm to obtain the sparse support set:

$$\min_{pq}\|\mathbf{U}_{pq}\|_1, \; \mathrm{s.\,t.} \; \left\|\mathbf{X}_{sv}^{pq} - \hat{\mathbf{A}}_t^{pq}\mathbf{U}_{pq}\right\|_F^2 \leq \varepsilon. \quad (11)$$

Using the optimization model expressed in Eq. (11) will cause large off-grid errors. To reduce the off-grid error, the first-order Taylor expansion is utilized to complete the preliminary angle estimation of each sub-array, expressed as:

$$\mathbf{a}_{tl}^q(\alpha_{tl}^q, \beta_{tl}^q) = \left(\mathbf{a}_{tl}^q\left(\gamma_{g,q}^l\right) + \frac{\partial\mathbf{a}_{tl}^q\left(\gamma_{g,q}^l\right)}{\partial\gamma_{g,q}^l}b_q^l \right)$$
$$\otimes \left(\mathbf{a}_{tl}^q\left(\eta_{g,q}^l\right) + \frac{\partial\mathbf{a}_{tl}^q\left(\eta_{g,q}^l\right)}{\partial\eta_{g,q}^l}c_q^l \right) \quad (12)$$

where $\gamma_{g,q}^l$, $\eta_{g,q}^l$ are the grid points closest to α_{tl}^q, β_{tl}^q, respectively. $b_q^l = \alpha_{tl}^q - \gamma_{g,q}^l$, $c_q^l = \beta_{tl}^q - \eta_{g,q}^l$ are the corresponding off-grid errors. Due to the orthogonality between the signal and the noise subspace, the optimal model Eq. (11) can be equivalent as [15]:

$$\mathop{\arg\min}_{b_q^l, c_q^l}\mathbf{h}_t^q\left(b_q^l, c_q^l\right) = \mathop{\arg\min}_{b_q^l, c_q^l}\left\|\mathbf{E}_t^{pqH}\mathbf{a}_{tl}^q(\alpha_{tl}^q\beta_{tl}^q)\right\|_2^2. \quad (13)$$

Thus the azimuth and elevation AoDs can be obtained.

$$\alpha_{tl}^q = \gamma_{g,q}^l + \hat{b}_q^l, \beta_t^l = \eta_{g,q}^l + \hat{c}_q^l. \quad (14)$$

Similarly, the azimuth and elevation AoDs can be obtained.

According to the estimated AoAs and AoDs, we can obtain the path gain by the least squares (LS) method [26]. Substitute to the estimated AoAs, AoDs and path gain, the channel matrix $\hat{\mathbf{H}}$ can be reconstructed by using Eq. (5), shown at the bottom of the page. The proposed algorithm can be summarized as Algorithm 1.

IV. SIMULATION ANALYSIS

In this section, simulated results based on the proposed algorithm is given. For comparison, the results of ADMM

$$\mathbf{H} = \sqrt{\frac{N_{S_t} \times N_{S_r}}{L}} \sum_{l=1}^{L} \begin{bmatrix} \mu_l^{11}\mathbf{a}_{rl}^1(\alpha_{rl}^1, \beta_{rl}^1)\mathbf{a}_{tl}^1(\alpha_{tl}^1, \beta_{tl}^1)^H & \cdots & \mu_l^{1S_t}\mathbf{a}_{rl}^1(\alpha_{rl}^1, \beta_{rl}^1)\mathbf{a}_{tl}^{S_t}\left(\alpha_{tl}^{S_t}, \beta_{tl}^{S_t}\right)^H \\ \vdots & \cdots & \vdots \\ \mu_l^{S_r 1}\mathbf{a}_{rl}^{S_r}\left(\alpha_{rl}^{S_r}, \beta_{rl}^{S_r}\right)\mathbf{a}_{tl}^1(\alpha_{tl}^1, \beta_{tl}^1)^H & \cdots & \mu_l^{S_r S_t}\mathbf{a}_{rl}^{S_r}\left(\alpha_{rl}^{S_r}, \beta_{rl}^{S_r}\right)\mathbf{a}_{tl}^{S_t}\left(\alpha_{tl}^{S_t}, \beta_{tl}^{S_t}\right)^H \end{bmatrix} \quad (5)$$

Algorithm 1 Sub-Array Based Channel Estimation Algorithm

Input: $\mathbf{Y}$, N_r, N_t, S_r, S_t, L, Δd.

Step 1: Perform singular value decomposition of the signal model to obtain the objective function;

Step 2: Construct the optimal model for channel estimation using Eq. (11);

Step 3: Find the grid point that is closest to the true angle according to Eq. (12);

Step 4: Calculate the off-grid error and approximate the true angle value using Taylor expansion;

Step 5: Repeat steps 1-4 to obtain the AoDs estimate for all sub-arrays;

Step 6: Calculate AoAs with the steps similar to 1-5;

Step 7: Obtain the path gain estimation by the LS method;

Step 8: Reconstruct the $\mathbf{H}$ according to Eq. (5).

Output: $\mathbf{H}$.

TABLE I
PARAMETER VALUE

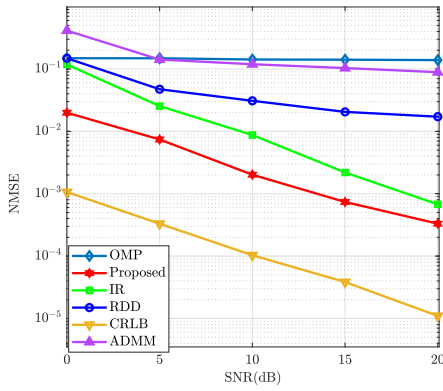| N_t	N_r	S_t	S_r	L	$\alpha_{rl}^p/\alpha_{tl}^q$	$\beta_{rl}^p/\beta_{tl}^q$	Δd
64/128/256	64/128/256	4	4	2/4/6	$[0, 2\pi]$	$[0, \pi]$	$\lambda/2$

Fig. 2. NMSE of the proposed algorithm with $N_t = N_r = 64$, $L = 4$. For comparison, the ADMM, IR, OMP algorithms are also given.

method [9], OMP method [10], iterative reweighting (IR)-based method [14], and reduced dimensional decomposition (RDD) method [16] are also given.

Here, the normalized mean square error (NMSE) is used to evaluate the performance of the proposed algorithm. NMSE is calculated as $\mathrm{E}[\|\hat{\mathbf{H}} - \mathbf{H}\|_F^2/\|\mathbf{H}\|_F^2]$, where $\hat{\mathbf{H}}$ represents the estimated channel matrix. In addition, the parameters used in the simulations are listed in Table I.

Evidently, Fig. 2 shows that our proposed scheme has the best NMSE performance compared with the other schemes. Due to the spherical wavefront, the RDD algorithm based on the plane wave model possesses lower performance than the proposed algorithm. Alternatively, the OMP method exploits the sparsity of the channel matrix to achieve the channel recovery. Owing to the limitation of the codebook size, OMP algorithm is inferior to the proposed algorithm. The ADMM method exploits the sparsity and low-rank properties of the channel to achieve a faster convergence. Due to the instability of convergence, the precision of the ADMM algorithm is limited. Compared with the IR algorithm, the proposed algorithm

TABLE II
COMPLEXITY AND TRAINING OVERHEAD

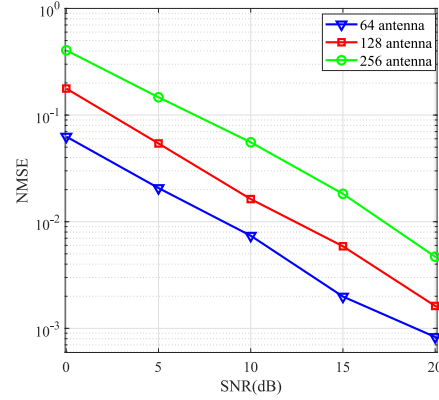| Algorithm	Complexity	Training overhead
	Analysis	
ADMM [9]	$O(N_r N_t)$	M
OMP [10]	$O(N_r N_t L^2)$	$\left(L^3/L_r\right)\log_2\left(G_r/L\right)$
IR [14]	$O(N_x N_y(N_r + N_t)L^2)$	MN_x
RDD [16]	$O(N_x(N_r + N_t)L^2)$	MN_x
Proposed	$O(N_x(N_r L^{S_r}/S_r + N_t L^{S_t}/S_t))$	$MN_x S_t$

Fig. 3. NMSE of the proposed algorithm with $N_t = N_r = 64, 128, 256$, $S_t = S_r = 4$, $L = 4$.

adopts the $l1$-norm with better robustness, and improves the accuracy. In order to facilitate the performance comparison, we also introduce Cramer-Rao lower bound [27]: (12), [28], which can be concluded that the proposed method can achieve the most ideal results.

Table II shows the complexity and training overhead of the above algorithm, where M, L_r and G_r are the number of time slots, RF chains and divided grids, respectively. The complexity of the ADMM method depends on the predefined angle grid and high-dimensional dictionary. The IR method uses the gradient descent to solve the off-grid problem, but its iteration cost is relatively high, resulting in higher complexity. It can be seen that when the number of paths and sub-arrays are small, the proposed algorithm possesses lower complexity. In addition, compared with IR algorithm and RDD algorithm, the proposed algorithm may require more training expenses. As the number of subarrays increases, the training expenditure will also increase. However, due to the small number of antennas in the sub-array, compared with other methods, fewer pilots can be allocated, and the training cost is moderate. Thus, the tradeoff between accuracy, complexity and number of training frames should be considered in the future work.

Progressively, Fig. 3 displays the NMSE of our scheme for different number of antennas, i.e., 64, 128 and 256. When the number of sub-arrays is fixed as 4, it can be seen that as the number of antennas increases, the performance of NMSE descends. The reason for this conclusion is that NMSE depends on the off-grid errors of the AoAs and AoDs. The equation of NMSE shows that the more antennas there are, the larger off-grid error will be.

Fig. 4 shows the NMSE of the proposed scheme with the number of paths set as 2, 4 and 6, respectively. It can be
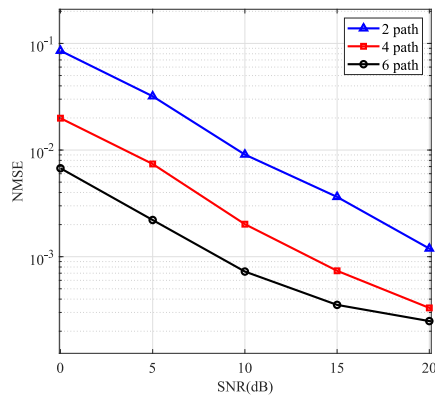
Fig. 4. NMSE with the number of paths $L = 2,4,6$.

seen that the higher the number of observed paths, the more accurate the estimated results. However, increasing the number of paths leads to increased complexity, and there is an inherent trade-off between the accuracy and complexity.

V. CONCLUSION

In this letter, a hybrid pre-coded mmWave massive MIMO system channel estimation scheme based on the spherical-wave model has been proposed. Relying on the characteristics of spherical wave propagation, the large antenna array have been divided into several sub-arrays, and each sub-array can be estimated separately. Firstly, a dimensionality reduction method has been used to reconstruct the signal, and the joint estimation of AoAs and AoDs has been transformed into separate estimation to reduce the complexity. Then, singular value decomposition has been used to distinguish the signal subspace from the noise subspace, and the sparse signal sets of each sub-array have been obtained via sparse signal reconstruction. Finally, the Taylor formula has been used for iteration to reduce the off-grid error and obtain the optimal value. Accuracy and complexity of the proposed algorithm have been compared with the other algorithms. Results have showed that the proposed scheme can obtain a better performance.

REFERENCES

[1] T. Kebede, Y. Wondie, J. Steinbrunn, H. B. Kassa, and K. T. Kornegay, "Precoding and beamforming techniques in mmWave-massive MIMO: Performance assessment," *IEEE Access*, vol. 10, pp. 16365–16387, Feb. 2022.
[2] C.-X. Wang et al., "On the road to 6G: Visions, requirements, key technologies, and testbeds," *IEEE Commun. Surveys Tuts.*, vol. 25, no. 2, pp. 905–974, 2nd Quart., 2023, doi: 10.1109/COMST.2023.3249835.
[3] Y. Song, Z. Gong, Y. Chen, and C. Li, "Efficient channel estimation for wideband millimeter wave massive MIMO systems with beam squint," *IEEE Trans. Commun.*, vol. 70, no. 5, pp. 3421–3435, May 2022.
[4] C.-X. Wang, J. Huang, H. Wang, X. Gao, X. You, and Y. Hao, "6G wireless channel measurements and models: Trends and challenges," *IEEE Veh. Technol. Mag.*, vol. 15, no. 4, pp. 22–32, Dec. 2020.
[5] S. A. Busari, K. M. S. Huq, S. Mumtaz, L. Dai, and J. Rodriguez, "Millimeter-wave massive MIMO communication for future wireless systems: A survey," *IEEE Commun. Surveys Tuts.*, vol. 20, no. 2, pp. 836–869, 2nd Quart., 2018.
[6] Y. Wang, Y. Zhang, Z. Tian, G. Leus, and G. Zhang, "Super-resolution channel estimation for arbitrary arrays in hybrid millimeter-wave massive MIMO systems," *IEEE J. Sel. Topics Signal Process.*, vol. 13, no. 5, pp. 947–960, Sep. 2019.
[7] K. Hassan, M. Masarra, M. Zwingelstein, and I. Dayoub, "Channel estimation techniques for millimeter-wave communication systems: Achievements and challenges," *IEEE Open J. Commun. Soc.*, vol. 1, pp. 1336–1363, Sep. 2020.
[8] F. Schweppe, "Evaluation of likelihood functions for Gaussian signals," *IEEE Trans. Inf. Theory*, vol. 11, no. 1, pp. 61–70, Jan. 1965.
[9] E. Vlachos, G. C. Alexandropoulos, and J. Thompson, "Massive MIMO channel estimation for millimeter wave systems via matrix completion," *IEEE Signal Process. Lett.*, vol. 25, no. 11, pp. 1675–1679, Nov. 2018.
[10] R. Mendez-Rial, C. Rusu, N. Gonzalez-Prelcic, A. Alkhateeb, and R. W. Heath, "Hybrid MIMO architectures for millimeter wave communications: Phase shifters or switches?" *IEEE Access*, vol. 4, pp. 247–267, Mar. 2016.
[11] A. Liao, Z. Gao, Y. Wu, H. Wang, and M.-S. Alouini, "2D unitary ESPRIT based super-resolution channel estimation for millimeter-wave massive MIMO with hybrid precoding," *IEEE Access*, vol. 5, pp. 24747–24757, Nov. 2017.
[12] Y. Han, S. Jin, C.-K. Wen, and X. Ma, "Channel estimation for extremely large-scale massive MIMO systems," *IEEE Wireless Commun. Lett.*, vol. 9, no. 5, pp. 633–637, May 2020.
[13] V. V. Ratnam and A. F. Molisch, "Periodic analog channel estimation aided beamforming for massive MIMO systems," *IEEE Trans. Wireless Commun.*, vol. 18, no. 3, pp. 1581–1594, Mar. 2019.
[14] C. Hu, L.-L. Dai, T. Mir, Z. Gao, and J. Fang, "Super-resolution channel estimation for mmWave massive MIMO with hybrid precoding," *IEEE Trans. Veh. Technol.*, vol. 67, no. 9, pp. 8954–8958, Sep. 2018.
[15] B. Qi, W. Wang, and B. Wang, "Off-grid compressive channel estimation for mm-Wave massive MIMO with hybrid precoding," *IEEE Commun. Lett.*, vol. 23, no. 1, pp. 108–111, Jan. 2019.
[16] R. Dai, Y. Liu, Q. Wang, Y. Yu, and X. Guo, "Channel estimation by reduced dimension decomposition for millimeter wave massive MIMO system," *Phys. Commun.*, vol. 44, Feb. 2021, Art. no. 101241.
[17] Y. Fu, C.-X. Wang, X. Fang, L. Yan, and S. Mclaughlin, "BER performance of spatial modulation systems under a non-stationary massive MIMO channel model," *IEEE Access*, vol. 8, pp. 44547–44558, Mar. 2020.
[18] S. Hou, Y. Wang, T. Zeng, and S. Wu, "Sparse channel estimation for spatial non-stationary massive MIMO channels," *IEEE Commun. Lett.*, vol. 24, no. 3, pp. 681–684, Mar. 2020.
[19] Z. Gao et al., "Data-driven deep learning based hybrid beamforming for aerial massive MIMO-OFDM systems with implicit CSI," *IEEE J. Sel. Areas Commun.*, vol. 40, no. 10, pp. 2894–2913, Oct. 2022.
[20] L. L. Magoarou, A. L. Calvez, and S. Paquelet, "Massive MIMO channel estimation taking into account spherical waves," in *Proc. IEEE Int. Workshop Signal Process. Adv. Wireless Commun. (SPAWC)*, Jul. 2019, pp. 1–5.
[21] M. Cui and L.-L. Dai, "Channel estimation for extremely large-scale MIMO: Far-field or near-field?" *IEEE Trans. Commun.*, vol. 70, no. 4, pp. 2663–2677, Apr. 2022.
[22] X.-H. Wei and L.-L. Dai, "Channel estimation for extremely large-scale massive MIMO: Far-field, near-field, or hybrid-field?" *IEEE Commun. Lett.*, vol. 26, no. 1, pp. 177–181, Jan. 2022.
[23] Y. Chen and Y.-C. Han, "Deep CNN-based spherical-wave channel estimation for terahertz ultra-massive MIMO systems," in *Proc. GLOBECOM IEEE Global Commun. Conf.*, Dec. 2020, pp. 1–6.
[24] Y. Chen, L. Yan, and Y.-C. Han, "Hybrid spherical- and planar-wave modeling and DCNN-powered estimation of terahertz ultra-massive MIMO channels," *IEEE Trans. Commun.*, vol. 69, no. 10, pp. 7063–7076, Oct. 2021.
[25] C. -X. Wang, Z. Lv, X. Gao, X. You, Y. Hao, and H. Haas, "Pervasive wireless channel modeling theory and applications to 6G GBSMs for all frequency bands and all scenarios," *IEEE Trans. Veh. Technol.*, vol. 71, no. 9, pp. 9159–9173, Sep. 2022.
[26] D. Fan et al., "Angle domain channel estimation in hybrid millimeter wave massive MIMO systems," *IEEE Trans. Wireless Commun.*, vol. 17, no. 12, pp. 8165–8179, Dec. 2018.
[27] S. Kay, "A fast and accurate single frequency estimator," *IEEE Trans. Acoust. Speech Signal Process.*, vol. 37, no. 12, pp. 1987–1990, Dec. 1989.
[28] Z. Gao et al., "Integrated sensing and communication with mmWave massive MIMO: A compressed sampling perspective," *IEEE Trans. Wireless Commun.*, vol. 22, no. 3, pp. 1745–1762, Mar. 2023.